PROCEEDINGS OF SCIENCE

Constraints on BSM particles from the absence of upward-going air showers in the Pierre Auger Observatory

Baobiao Yue[a,*] **for the Pierre Auger Collaboration**[b]

[a] *Bergische Universität Wuppertal, Department of Physics, Gaußstraße 20, Wuppertal, Germany*
[b] *Observatorio Pierre Auger, Av. San Martín Norte 304, 5613 Malargüe, Argentina*
Full author list: https://www.auger.org/archive/authors_icrc_2023.html

E-mail: bayue@uni-wuppertal.de, spokespersons@auger.org

The Fluorescence Detector (FD) of the Pierre Auger Observatory has a large exposure to search for upward-going showers. Constraints have been recently obtained by using 14 years of FD data searching for upward-going showers in the zenith angle range $[110°, 180°]$. In this work, we translate these bounds to upper limits of a possible flux of ultra high energy tau-leptons escaping from the Earth into the atmosphere. Such a mechanism could explain the observation of "anomalous pulses" made by ANITA, that indicated the existence of upward-going air showers with energies above 10^{17} eV. As tau neutrinos would be absorbed within the Earth at the deduced angles and energies, a flux of upward-going taus could only be resulted from an unknown type of ultra high energy Beyond Standard Model particle penetrating the Earth with little attenuation, and then creating tau-leptons through interactions within a maximum depth of about 50 km before exiting. We test classes of such models in a generic way and determine upper flux limits of ultra high energy BSM particles as a function of their unknown cross section with matter.

38th International Cosmic Ray Conference (ICRC2023)
26 July – 3 August, 2023
Nagoya, Japan

*Speaker

PoS(ICRC2023)1095

1. Introduction

The Antarctic Impulsive Transient Antenna (ANITA) was designed to search for ultra high energy (UHE[1]) neutrinos by detecting the radio pulses produced as the neutrinos transit the Antarctic ice. Recently, ANITA reported the detection of two anomalous events appearing from below the horizon with shower energies exceeding 0.2 EeV at zenith angles $117.4° \pm 0.3°$ [1] and $125.0° \pm 0.3°$ [2], respectively. Although consistent with the characteristics of a τ lepton cascade, the problem in interpreting these events as due to a ν_τ is that the Standard Model (SM) weak interaction is sufficiently strong at these energies to render the Earth practically opaque to neutrinos, with a transmission probability below about 10^{-5}. A dedicated analysis [3] of these two events has been given assuming a diffuse $\nu_\tau/\bar{\nu}_\tau$ flux detected via τ-lepton induced air showers within the bounds of standard model uncertainties. By comparing an estimate of the exposure to tau neutrinos with the Pierre Auger Observatory [4, 5] and IceCube [6] it is found that a diffuse tau neutrino flux would have to be at least two orders of magnitude above current bounds to explain these two events within the SM, thus excluding a diffuse cosmic $\nu_\tau/\bar{\nu}_\tau$ origin. As no other explanations are allowed within the SM, these events have attracted a lot of attention and several Beyond Standard Model (BSM) hypotheses have been postulated.

Upward-going showers in the atmosphere can be produced by BSM particles propagating through the Earth and producing a tau lepton before exiting. Such interpretations include sterile neutrino mixing [7, 8], heavy dark matter [9, 10], stau decays [11, 12], and $L_e - L_\tau$ gauge interaction [13] etc.. Given the transcendence that the discovery of any of these new mechanisms would have, a search for upward-going air showers in the Pierre Auger Observatory has been launched. The results of this search are being reported elswhere at this conference [26].

No excess of events above background has been found despite the larger exposure of the Pierre Auger Fluorescence Detector (FD). This non-observation was used to set upper limits to the flux of upward-going showers. The study presented here, builds on this search and translates those upper limits to upper bounds on fluxes of BSM particles propagating through the Earth and creating tau particles that could be detected as upward-going air showers. Since the interaction cross section of such particles is not known, we treat this as a free parameter and express the upper bounds in terms of $\Phi_{\text{BSM}} \cdot \sigma_{\text{BSM-matter}}$.

2. The reduced cross section BSM model

In the SM, the cross section of neutrinos grows with energy so that Earth becomes opaque above $E_\nu \approx 10^{15}$ eV [14]. However, if BSM particles do exist with an interaction cross section lower than that of neutrinos and if they can produce tau leptons through interactions with matter, they may explain the "anomalous pulses" seen by ANITA. Therefore, we construct a BSM model with some simple assumptions for the purpose of general usage. The model assumes a diffuse flux of BSM particles that reach the Earth isotropically and interact with matter at variable cross section. A BSM particle interaction can produce a tau lepton, which propagates through the Earth to the surface and develops an upward-going shower. Currently, the model only has a tau generation interaction. The energy transfer from BSM to tau lepton can be simply assumed with fixed proportion, such as

[1]Ultra high energy means $E > 100$ PeV.

100%, 50% etc., instead of energy transfer distribution known from tau neutrinos [15]. With these simple assumptions, we can include several BSM scenarios in this study. Some other cases in which BSM particles decay or have other interactions without tau generation are deferred for later studies.

2.1 Propagation and tau generation in the Earth

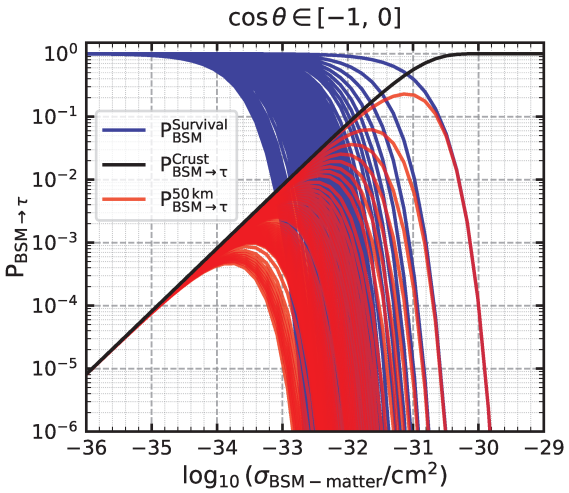

Figure 1: The probability of the reduced cross section BSM to produce tau in last 50 km underground with constant matter density 2.7 g/cm^3. Different curve in the same color is given by different $\cos\theta$ with equal interval. $P^{Crust}_{BSM\to\tau}$ is the same for different $\cos\theta$ due to the same matter density and τ generation length.

Compared to SM neutrinos, BSM particles with reduced cross sections can traverse the Earth with higher probability. However, a very low cross section will reduce the interaction and thereby tau creation probability in the crust of the Earth below the Observatory. UHE tau leptons can propagate through up to 50 kilometer of rock [16] and escape into the atmosphere before being absorbed. Therefore, the product of the survival probability through an Earth chord to reach the fiducial volume 50 km before exiting into the atmosphere ($P^{Survival}_{BSM}$) and the tau generation probability within the last 50 km of crust ($P^{Crust}_{BSM\to\tau}$) yields the total probability ($P^{50\,km}_{BSM\to\tau}$) for the BSM particle to produce a tau, that may exit into the atmosphere to produce an upward-going air shower. We find that tau leptons with energies below 10^{21} eV cannot exit into the atmosphere unless they are produced within the last 50 km of rock.

To calculate the BSM survival probability through the Earth for a given zenith angle, the Earth density profile is needed. For this purpose, we simplify the Preliminary Reference Earth Model (PREM) [17] with slab approximation, which assumes a constant density in each Earth layer. Based on this approximation, the BSM survival probability through the Earth is given by:

$$P^{Survival}_{BSM} = \exp\left(-\frac{N_A\cdot\sigma_{BSM-matter}}{M}\sum_i^{n(\theta)} l_i(\theta)\cdot\rho_i\right), \tag{1}$$

where $N_A = 6.02214\cdot 10^{23}$ is the Avogadro number, $\sigma_{BSM-matter}$ represents BSM interaction cross section for an isoscalar target, M $\approx$ 1g/mol stands for the molar mass of isoscalar targets, $n(\theta)$ is the total number of layers crossed by the trajectory chord from the entry point at Earth to 50 km of rock [2], θ is the zenith angle measured at entry or exit points, and $l_i(\theta)$ and ρ_i are respectively the propagation length and matter density in each layer. The tau generation probability in the last

[2]Under the assumption that the Earth is spherical, the chord length for some horizontal zenith angles will be less than 50 km. We will increase the chord length according to the actual geographical situation. For example, when zenith angle is 90°, we still consider the chord length to be 50 km in the Auger Observatory site.

50 km of crust is given by:

$$P^{\text{Crust}}_{\text{BSM}\to\tau} = 1 - \exp\left(-\frac{N_A \cdot \sigma_{\text{BSM-matter}}}{M} \cdot l \cdot \rho\right), \tag{2}$$

where $l = 50$ km is the total length for tau generation below the surface of the Earth and ρ is 2.7 g/cm^3. For a constant density approximation in the last 50 km of the Earth's crust,the interaction probability is an exponential of the length l. When the cross section becomes less than about 10^{-31} cm^2, the interaction length exceeds 50 km in rock so that tau generation can be treated as a uniform distribution along the BSM propagation path in the fiducial volume.

The total probability for the BSM to produce a tau lepton in the fiducial volume can be written as:

$$\mathrm{P}^{50\,\text{km}}_{\text{BSM}\to\tau} = \mathrm{P}^{\text{Survival}}_{\text{BSM}} \cdot \mathrm{P}^{\text{Crust}}_{\text{BSM}\to\tau} \cdot \tag{3}$$

Figure 1 shows the total probability as a function of cross section for different values of $\cos\theta$. For a fixed cross section, we find the lower the BSM propagation length, the larger the tau generation probability. Furthermore, we can find the cross section that gives a maximum probability to produce tau with a specific angle.

Once the tau generation probability from BSM is known, we can obtain the tau generation integrated flux in the last 50 km of the Earth's crust, Φ^G_τ, written by:

$$\Phi^G_\tau(E,\theta) = \Phi_{\text{BSM}}(E,\theta) \cdot \mathrm{P}^{50\,\text{km}}_{\text{BSM}\to\tau}(E,\theta)\,, \tag{4}$$

where $\Phi_{\text{BSM}}(E,\theta)$ is the incident flux of BSM particles and $\mathrm{P}^{50\,\text{km}}_{\text{BSM}\to\tau}$ is the probability expressed in Eq. 3 to produce a tau in the last 50 km of crust. The energy fraction that is transferred from BSM to tau particles is assumed to be 100%.

3. Tau induced air shower

Once a tau is produced in the Earth, it will propagate and suffer energy losses and eventually may decay still within the Earth. If it survives to the surface, it may decay in the atmosphere and generate an upward-going air shower. In this section, we discuss the tau propagation in the Earth and air and its decay in the atmosphere that induces an air shower.

3.1 Tau propagation

When a tau lepton propagates in the Earth, its energy loss can be approximated by:

$$-\left\langle \frac{\mathrm{d}E_\tau}{\mathrm{d}l} \right\rangle = \alpha + \beta E_\tau\,, \tag{5}$$

where α corresponds to ionization losses and the term proportional to energy is due to bremsstrahlung, pair production, and photonuclear processes with β independent of energy. At the energies discussed here, the dominant process of tau energy loss are photonuclear interactions. In this study, we use the ALLM model[3] [18] for photonuclear process by default. When a tau propagates, not only does it lose energy, but its decay length is correspondingly shortened. The tau decay length can be

[3]Another popular model is ASW [19].

expressed as $c\tau \cdot E_\tau/m_\tau$, where E_τ is tau energy, m_τ is the rest mass of the tau (1.777 GeV/c^2), and τ is its lifetime $2.903 \cdot 10^{-13}$ s. The program designed for simulations of tau propagation is based on NuTauSim [16]. If a tau survives to the surface from the Earth, it will propagate in the atmosphere practically without energy losses due to the low density of air and eventually will decay and can generate an upward-going shower.

3.2 Tau decay

The tau has 35.21% leptonic and 64.79% hadronic decays [20]. The secondary particles of tau decay comprise of: $e^\pm$, $\nu_e/\bar{\nu}_e$, $\mu^\pm$, $\nu_\mu/\bar{\nu}_\mu$, $\nu_\tau/\bar{\nu}_\tau$,$\pi^\pm$, π^0, $K^\pm$, $K^0/\bar{K}^0$, $K^0_{L/S}$ and γ, where π^0 ($\tau = 8.4 \cdot 10^{-17}$s) and K^0_S ($\tau = 8.953 \cdot 10^{-11}$s) will decay immediately. A π^0 will decay to 2γ's and K^0_S will decay to $\pi^+\pi^-$ or $2\pi^0$, with the latter decaying immediately again to 2γ's. Tau decay simulations are directly obtained from TAUOLA [21] which also gives access to the four momenta of the secondary particles.

Neutrinos and muons are invisible both to the Auger FD and ANITA. Therefore, we only need to consider the energy deposited by $e^\pm$, $\pi^\pm$, $K^\pm$, $K^0/\bar{K}^0$, K^0_L and γ in the air. According to the simulation results from a specially designed program, the double differential distribution of tau decay can be obtained in shower energy and slant depth plane. This is easily converted into a distribution in shower energy and altitude above ground level using a model for the density in the atmosphere.

4. Upward-going showers with the fluorescence detector in Pierre Auger Observatory

A dedicated search for upward-going showers using the FD of the Pierre Auger Observatory resulted in one event consistent with an expected background of 0.27 ± 0.12 which is consistent with the expectation from mis-reconstructions of regular cosmic ray showers [26]. The results of this search can be converted into strong constraints on BSM scenarios, such as were put forward to explain the observation of "anomalous pulses" made with ANITA. Here, we present results making the assumption that the BSM particles follow a power law energy spectrum E^{-2} for the considered energy range. We study the constraints on tau production which can be of relevance for any explanation of the anomalous upward-going showers based on a BSM scenario that produces tau leptons. The results obtained can be thus applied to any of such models.

The left plot in Figure 2 shows the upper limits on taus generated in the fiducial volume below ground as a function of their production energy. Several limits have been obtained corresponding to the three different zenith angle bins in which the search has been split, $[110°, 124.2°]$, $[124.2°, 141.3°]$, $[141.3°, 180°]$ and to the combination of all three bins, $[110°, 180°]$. Additionally, we can also place a limit on the flux of taus reaching the ground and exiting Earth. This is shown in the right plot of Figure 2. The difference between the upper limits of tau generation and surface tau in Figure 2 is caused by the fact that not all taus generated in the fiducial volume exit Earth to enter the atmosphere. These different representations of the upper limits can be used to constrain any BSM model that produces taus in the Earth.

Since the cross section of BSM particles with matter to produce taus is unknown, we adopt two simple strategies to include more cases of BSM scenarios. The first strategy is a scenario which

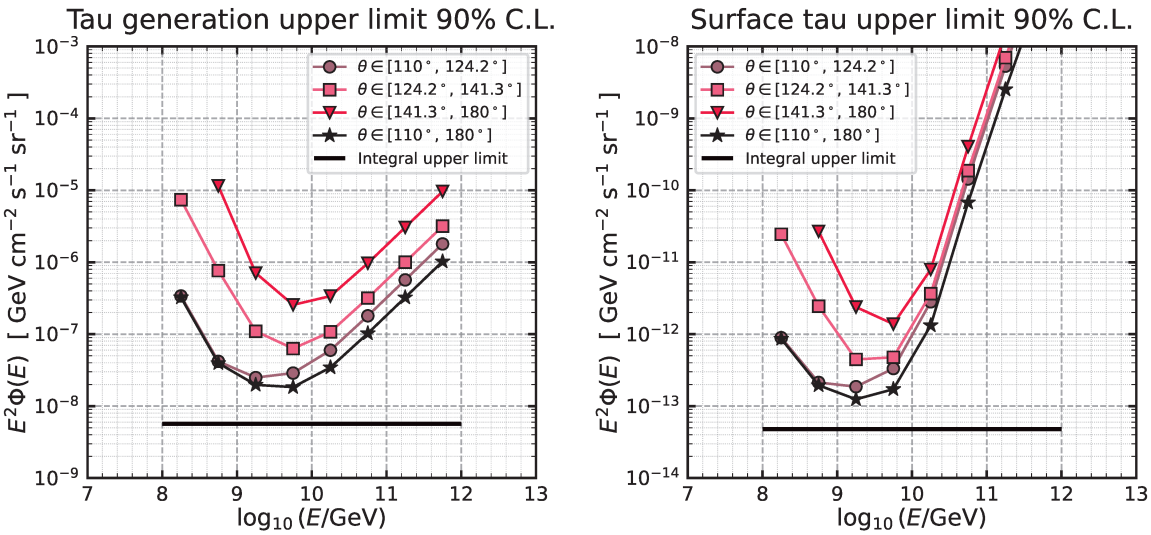

Figure 2: Left: tau generation upper limit with 90% C.L. with FD. Right: tau surface flux upper limit with 90% C.L.. These three zenith angle sub-ranges have the equal values of $\Delta \cos\theta$ in $[110°,\ 180°]$.

assumes a constant cross section at all relevant energies. The second strategy is based on a model in which the cross section of the BSM particle mimics a neutrino charged current interaction with the same energy dependence but a normalization scaled by a fixed factor ranging from 1 to 10^{-5}. Figure 3 presents the upper flux limits obtained for BSM particles. In the top plots, the cross section is assumed to be fixed and the limits are plotted as a function of the cross section. The integral limits are shown on the left plot and the differential limits obtained by integrating in half a decade bin is plotted on the right as a function of BSM energy. Equivalent integral and differential flux limits are plotted on the bottom of Figure 3 in the scenario in which the cross section is scaled down w.r.t. the neutrino charged current cross section. The factor used to scale the cross section scans the range between 10^{-5} and 1 for the integral flux limit on the left and the differential limit on the right is plotted for factors corresponding to integer powers of 10 in the same range. The strongest limit for the BSM flux is obtained for a fixed cross section of order 10^{-33} cm^2 in the first scenario of an energy independent cross section. In the second scenario the strongest flux limit is obtained for a cross section that is 3% of the neutrino charged current cross section. In both scenarios the 90% C.L. limit of the flux is at the level of $3 \cdot 10^{-6}$ GeV cm^{-2} s^{-1} sr^{-1} for the integral flux and of order 10^{-5} GeV cm^{-2} s^{-1} sr^{-1} for the differential fluxes.

As shown in Figure 3, we can also utilize the Earth-Skimming (ES) channel [25] in the Surface Detector (SD) of the Auger Observatory to validate the diffuse flux of the reduced cross section BSM particles with zenith angle in $[90°,\ 95°]$. Given the almost 100 % duty cycle of the SD, we find that the ES channel can provide the strongest limit on the diffuse flux for this kind of BSM particles, despite its limited solid angle.

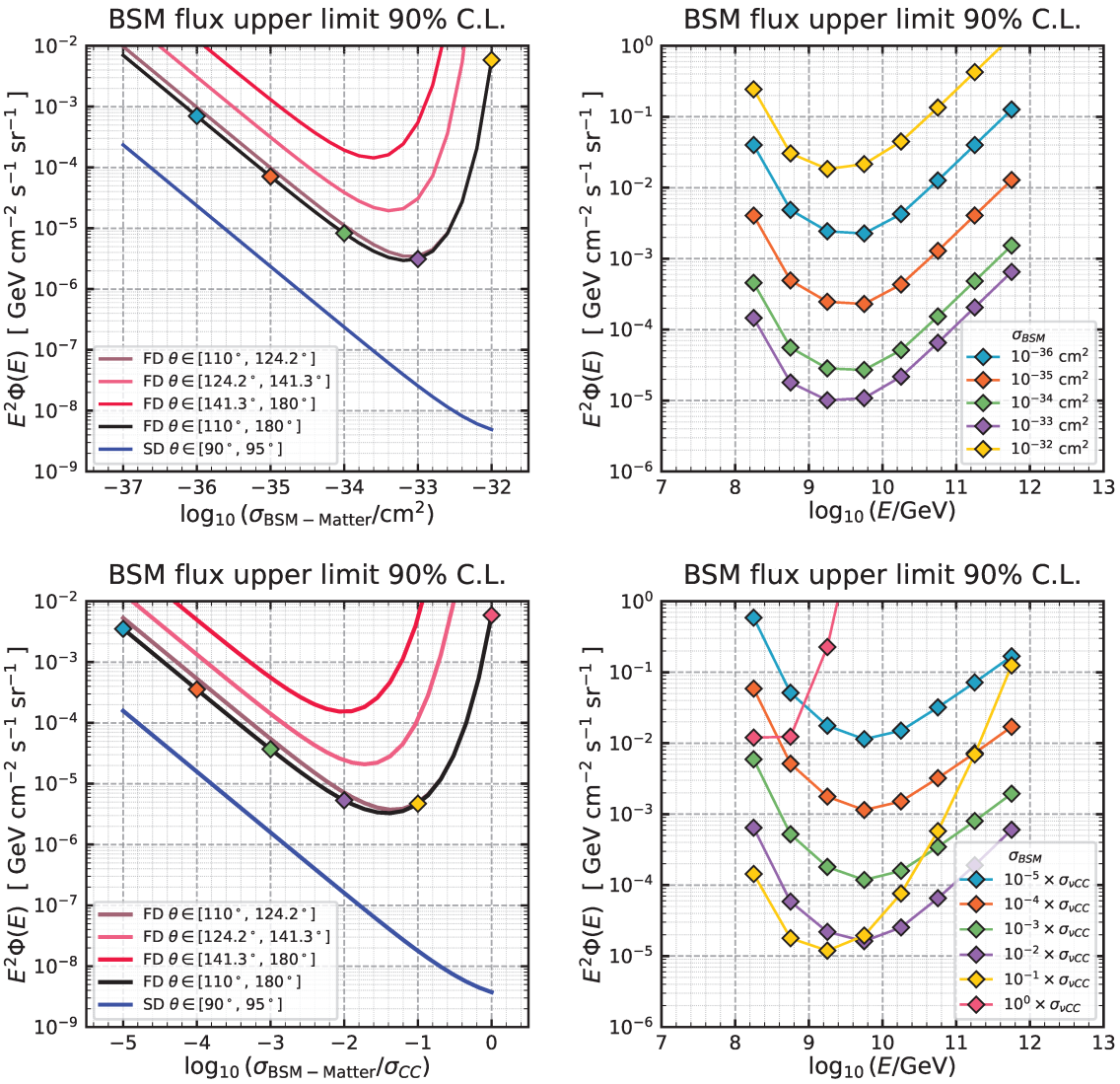

Figure 3: Upper: upper limits of BSM flux for the constant cross section BSM scenarios. Lower: upper limit of BSM flux for the scaled SM $\sigma_{\nu\mathrm{CC}}$. The left plots are the integral upper limits of BSM flux in energy range $[10^{17}, 10^{21}]$ eV. The right plots are the differential upper limits of BSM flux in zenith range $[110^\circ, 180^\circ]$.

5. Conclusions

ANITA observed two upward-going events which could be due to tau leptons decaying in the atmosphere but which are not consistent with neutrino interactions within the SM of particle physics. We investigate two model independent BSM scenarios in which they produce tau leptons inside the Earth with a cross section which is assumed to be constant or to be a fraction of the neutrino charged current interaction. We have obtained flux limits for these BSM particles assuming an E^{-2} spectrum using the results of a search for upward-going showers with the Pierre Auger Observatory. Bounds are obtained in the three zenith angle bins used for the search and combining them all and are presented in integral and differential form. We find that the strongest constraint can be set to

about $3 \cdot 10^{-6}$ GeV cm^{-2} s^{-1} sr^{-1} (90% C.L.) when BSM cross section is about 10^{-33} cm^2 or 3% of the SM neutrino charged current cross section. Since the exposure to upward-going showers in the FD is greater than the one of ANITA in the energy range $[10^{17}, 10^{19}]$ eV and at corresponding zenith angles [26], many models with SM tau production from BSM proposed to explain the observation of "anomalous pulses" made with ANITA could be ruled out. Furthermore, the ES channel of the SD provides even stronger constraints on the diffuse flux of BSM particles of reduced cross section. Thus, the combination of FD and SD observations enables us to provide the strongest presently available constraints on BSM particles producing taus by interactions in the Earth.

References

[1] P. W. Gorham *et al.* [ANITA collaboration], *Phys. Rev. Lett.* **117** (2016) 071101.
[2] P.W. Gorham *et al.* [ANITA collaboration], *Phys. Rev. Lett.* **121** (2018) 161102.
[3] A. Romero-Wolf *et al.*, *Phys. Rev. D* **99** (2019) 063011, arXiv: 1811.07261.
[4] A. Aab *et al.* [Pierre Auger Collaboration], *Phys. Rev. D* **91** (2015) 092008.
[5] A. Aab *et al.* [Pierre Auger Collaboration], *JCAP* **10** (2019) 022.
[6] M. G. Aartsen *et al.* [IceCube Collaboration], *Phys. Rev. Lett.* **117** (2016) 241101.
[7] G.-y. Huang, *Phys. Rev. D* **98** (2018) 043019, arXiv: 1804.05362 [hep-ph].
[8] John F. Cherry and Ian M. Shoemaker, *Phys. Rev. D* **99** (2019) 063016, arXiv: 1802.01611 [hep-ph].
[9] Luis A. Anchordoqui, Vernon Barger, John G. Learned, Danny Marfatia, and Thomas J. Weiler, *LHEP* **1.1**, pp. 13–16 (2018), arXiv: 1803.11554 [hep-ph].
[10] Emilian Dudas, Tony Gherghetta, Kunio Kaneta, Yann Mambrini, and Keith A. Olive, *Phys. Rev. D* **98** (2018) 015030 , arXiv: 1805.07342 [hep-ph].
[11] Amy Connolly, Patrick Allison, and Oindree Banerjee, arXiv: 1807.08892 [astro-ph.HE].
[12] Derek B. Fox, Steinn Sigurdsson, Sarah Shandera, Peter Mészáros, Kohta Murase, Miguel Mostafá, and Stephane Coutu, arXiv: 1809.09615 [astro-ph.HE].
[13] A. Esmaili and Y. Farzan, *JCAP* **12** (2019) 017, arXiv: 1909.07995.
[14] Amanda Cooper-Sarkar, Philipp Mertsch, Subir Sarkar, arXiv:1106.3723 [hep-ph]
[15] Lai, H., Huston, J., Kuhlmann, S. *et al.*, *Eur. Phys. J. C* **12** (2000) 375–392 . https://doi.org/10.1007/s100529900196
[16] Jaime Alvarez-Muñiz, Washington R. Carvalho, Jr., Kévin Payet, Andrés Romero-Wolf, Harm Schoorlemmer, and Enrique Zas, *Phys. Rev. D* **97** (2018) 023021
[17] Adam Dziewonski, in The Encyclopedia of Solid Earth Geophysics, edited by David E. James (Van Nostrand Reinhold, New York, 1989), p. 331.
[18] Halina A., Aharon L., arXiv:hep-ph/9712415.
[19] Néstor Armesto, Carlos A. Salgado, and Urs Achim Wiedemann, Phys. Rev. Lett. **94** (2005) 022002
[20] R.L. Workman *et al.* [Particle Data Group], *Prog. Theor. Exp. Phys* (2022) 083C01.
[21] N. Davidson *et al.*, In: Computer Physics Communications 183.3 (Mar. 2012), pp. 821–843. issn: 0010-4655.
[22] https://pdg.lbl.gov/2014/AtomicNuclearProperties/HTML/air_dry_1_atm.html
[23] T. Pierog *et al.*, In: *Nucl. Phys. B Proc. Suppl.* **151** (2006), pp. 159–162.
[24] Amanda Cooper-Sarkar, Philipp Mertsch, Subir Sarkar, arXiv:1106.3723 [hep-ph]
[25] A. Aab *et al.*, *JCAP* **10**(2019) 022.
[26] Emanuele De Vito for the [Pierre Auger Collaboration], "Constraints on upward-going air showers using the Pierre Auger Observatory data", PoS(ICRC2023)1099

The Pierre Auger Collaboration

A. Abdul Halim[13], P. Abreu[72], M. Aglietta[54,52], I. Allekotte[1], K. Almeida Cheminant[70], A. Almela[7,12], R. Aloisio[45,46], J. Alvarez-Muñiz[79], J. Ammerman Yebra[79], G.A. Anastasi[54,52], L. Anchordoqui[86], B. Andrada[7], S. Andringa[72], C. Aramo[50], P.R. Araújo Ferreira[42], E. Arnone[63,52], J. C. Arteaga Velázquez[67], H. Asorey[7], P. Assis[72], G. Avila[11], E. Avocone[57,46], A.M. Badescu[75], A. Bakalova[32], A. Balaceanu[73], F. Barbato[45,46], A. Bartz Mocellin[85], J.A. Bellido[13,69], C. Berat[36], M.E. Bertaina[63,52], G. Bhatta[70], M. Bianciotto[63,52], P.L. Biermann[h], V. Binet[5], K. Bismark[39,7], T. Bister[80,81], J. Biteau[37], J. Blazek[32], C. Bleve[36], J. Blümer[41], M. Boháčová[32], D. Boncioli[57,46], C. Bonifazi[8,26], L. Bonneau Arbeletche[21], N. Borodai[70], J. Brack[j], P.G. Brichetto Orchera[7], F.L. Briechle[42], A. Bueno[78], S. Buitink[15], M. Buscemi[47,61], M. Büsken[39,7], A. Bwembya[80,81], K.S. Caballero-Mora[66], S. Cabana-Freire[79], L. Caccianiga[59,49], I. Caracas[38], R. Caruso[58,47], A. Castellina[54,52], F. Catalani[18], G. Cataldi[48], L. Cazon[79], M. Cerda[10], A. Cermenati[45,46], J.A. Chinellato[21], J. Chudoba[32], L. Chytka[33], R.W. Clay[13], A.C. Cobos Cerutti[6], R. Colalillo[60,50], A. Coleman[90], M.R. Coluccia[48], R. Conceição[72], A. Condorelli[37], G. Consolati[49,55], M. Conte[56,48], F. Convenga[41], D. Correia dos Santos[28], P.J. Costa[72], C.E. Covault[84], M. Cristinziani[44], C.S. Cruz Sanchez[3], S. Dasso[4,2], K. Daumiller[41], B.R. Dawson[13], R.M. de Almeida[28], J. de Jesús[7,41], S.J. de Jong[80,81], J.R.T. de Mello Neto[26,27], I. De Mitri[45,46], J. de Oliveira[17], D. de Oliveira Franco[21], F. de Palma[56,48], V. de Souza[19], E. De Vito[56,48], A. Del Popolo[58,47], O. Deligny[34], N. Denner[32], L. Deval[41,7], A. di Matteo[52], M. Dobre[73], C. Dobrigkeit[21], J.C. D'Olivo[68], L.M. Domingues Mendes[72], J.C. dos Anjos, R.C. dos Anjos[25], J. Ebr[32], F. Ellwanger[41], M. Emam[80,81], R. Engel[39,41], I. Epicoco[56,48], M. Erdmann[42], A. Etchegoyen[7,12], C. Evoli[45,46], H. Falcke[80,82,81], J. Farmer[89], G. Farrar[88], A.C. Fauth[21], N. Fazzini[e], F. Feldbusch[40], F. Fenu[41,d], A. Fernandes[72], B. Fick[87], J.M. Figueira[7], A. Filipčič[77,76], T. Fitoussi[41], B. Flaggs[90], T. Fodran[80], T. Fujii[89,f], A. Fuster[7,12], C. Galea[80], C. Galelli[59,49], B. García[6], C. Gaudu[38], H. Gemmeke[40], F. Gesualdi[7,41], A. Gherghel-Lascu[73], P.L. Ghia[34], U. Giaccari[48], M. Giammarchi[49], J. Glombitza[42,g], F. Gobbi[10], F. Gollan[7], G. Golup[1], M. Gómez Berisso[1], P.F. Gómez Vitale[11], J.P. Gongora[11], J.M. González[1], N. González[7], I. Goos[1], D. Góra[70], A. Gorgi[54,52], M. Gottowik[79], T.D. Grubb[13], F. Guarino[60,50], G.P. Guedes[22], E. Guido[44], S. Hahn[39], P. Hamal[32], M.R. Hampel[7], P. Hansen[3], D. Harari[1], V.M. Harvey[13], A. Haungs[41], T. Hebbeker[42], C. Hojvat[e], J.R. Hörandel[80,81], P. Horvath[33], M. Hrabovský[33], T. Huege[41,15], A. Insolia[58,47], P.G. Isar[74], P. Janecek[32], J.A. Johnsen[85], J. Jurysek[32], A. Kääpä[38], K.H. Kampert[38], B. Keilhauer[41], A. Khakurdikar[80], V.V. Kizakke Covilakam[7,41], H.O. Klages[41], M. Kleifges[40], F. Knapp[39], N. Kunka[40], B.L. Lago[16], N. Langner[42], M.A. Leigui de Oliveira[24], Y Lema-Capeans[79], V. Lenok[39], A. Letessier-Selvon[35], I. Lhenry-Yvon[34], D. Lo Presti[58,47], L. Lopes[72], L. Lu[91], Q. Luce[39], J.P. Lundquist[76], A. Machado Payeras[21], M. Majercakova[32], D. Mandat[32], B.C. Manning[13], P. Mantsch[e], S. Marafico[34], F.M. Mariani[59,49], A.G. Mariazzi[3], I.C. Mariş[14], G. Marsella[61,47], D. Martello[56,48], S. Martinelli[41,7], O. Martínez Bravo[64], M.A. Martins[79], M. Mastrodicasa[57,46], H.J. Mathes[41], J. Matthews[a], G. Matthiae[62,51], E. Mayotte[85,38], S. Mayotte[85], P.O. Mazur[e], G. Medina-Tanco[68], J. Meinert[38], D. Melo[7], A. Menshikov[40], C. Merx[41], S. Michal[33], M.I. Micheletti[5], L. Miramonti[59,49], S. Mollerach[1], F. Montanet[36], L. Morejon[38], C. Morello[54,52], A.L. Müller[32], K. Mulrey[80,81], R. Mussa[52], M. Muzio[88], W.M. Namasaka[38], S. Negi[32], L. Nellen[68], K. Nguyen[87], G. Nicora[9], M. Niculescu-Oglinzanu[73], M. Niechciol[44], D. Nitz[87], D. Nosek[31], V. Novotny[31], L. Nožka[33], A Nucita[56,48], L.A. Núñez[30], C. Oliveira[19], M. Palatka[32], J. Pallotta[9], S. Panja[32], G. Parente[79], T. Paulsen[38], J. Pawlowsky[38], M. Pech[32], J. Pękala[70], R. Pelayo[65], L.A.S. Pereira[23], E.E. Pereira Martins[39,7], J. Perez Armand[20], C. Pérez Bertolli[7,41], L. Perrone[56,48], S. Petrera[45,46], C. Petrucci[57,46], T. Pierog[41], M. Pimenta[72], M. Platino[7], B. Pont[80], M. Pothast[81,80], M. Pourmohammad Shahvar[61,47], P. Privitera[89], M. Prouza[32], A. Puyleart[87], S. Querchfeld[38], J. Rautenberg[38], D. Ravignani[7], M. Reininghaus[39], J. Ridky[32], F. Riehn[79], M. Risse[44], V. Rizi[57,46], W. Rodrigues de Carvalho[80], E. Rodriguez[7,41], J. Rodriguez Rojo[11], M.J. Roncoroni[7], S. Rossoni[43], M. Roth[41], E. Roulet[1], A.C. Rovero[4], P. Ruehl[44], A. Saftoiu[73], M. Saharan[80], F. Salamida[57,46], H. Salazar[64], G. Salina[51], J.D. Sanabria Gomez[30], F. Sánchez[7], E.M. Santos[20], E. Santos[32],

F. Sarazin[85], R. Sarmento[72], R. Sato[11], P. Savina[91], C.M. Schäfer[41], V. Scherini[56,48], H. Schieler[41], M. Schimassek[34], M. Schimp[38], F. Schlüter[41], D. Schmidt[39], O. Scholten[15,i], H. Schoorlemmer[80,81], P. Schovánek[32], F.G. Schröder[90,41], J. Schulte[42], T. Schulz[41], S.J. Sciutto[3], M. Scornavacche[7,41], A. Segreto[53,47], S. Sehgal[38], S.U. Shivashankara[76], G. Sigl[43], G. Silli[7], O. Sima[73,b], F. Simon[40], R. Smau[73], R. Šmída[89], P. Sommers[k], J.F. Soriano[86], R. Squartini[10], M. Stadelmaier[32], D. Stanca[73], S. Stanič[76], J. Stasielak[70], P. Stassi[36], S. Strähnz[39], M. Straub[42], M. Suárez-Durán[14], T. Suomijärvi[37], A.D. Supanitsky[7], Z. Svozilikova[32], Z. Szadkowski[71], A. Tapia[29], C. Taricco[63,52], C. Timmermans[81,80], O. Tkachenko[41], P. Tobiska[32], C.J. Todero Peixoto[18], B. Tomé[72], Z. Torrès[36], A. Travaini[10], P. Travnicek[32], C. Trimarelli[57,46], M. Tueros[3], M. Unger[41], L. Vaclavek[33], M. Vacula[33], J.F. Valdés Galicia[68], L. Valore[60,50], E. Varela[64], A. Vásquez-Ramírez[30], D. Veberič[41], C. Ventura[27], I.D. Vergara Quispe[3], V. Verzi[51], J. Vicha[32], J. Vink[83], J. Vlastimil[32], S. Vorobiov[76], C. Watanabe[26], A.A. Watson[c], A. Weindl[41], L. Wiencke[85], H. Wilczyński[70], D. Wittkowski[38], B. Wundheiler[7], B. Yue[38], A. Yushkov[32], O. Zapparrata[14], E. Zas[79], D. Zavrtanik[76,77], M. Zavrtanik[77,76]

[1] Centro Atómico Bariloche and Instituto Balseiro (CNEA-UNCuyo-CONICET), San Carlos de Bariloche, Argentina
[2] Departamento de Física and Departamento de Ciencias de la Atmósfera y los Océanos, FCEyN, Universidad de Buenos Aires and CONICET, Buenos Aires, Argentina
[3] IFLP, Universidad Nacional de La Plata and CONICET, La Plata, Argentina
[4] Instituto de Astronomía y Física del Espacio (IAFE, CONICET-UBA), Buenos Aires, Argentina
[5] Instituto de Física de Rosario (IFIR) – CONICET/U.N.R. and Facultad de Ciencias Bioquímicas y Farmacéuticas U.N.R., Rosario, Argentina
[6] Instituto de Tecnologías en Detección y Astropartículas (CNEA, CONICET, UNSAM), and Universidad Tecnológica Nacional – Facultad Regional Mendoza (CONICET/CNEA), Mendoza, Argentina
[7] Instituto de Tecnologías en Detección y Astropartículas (CNEA, CONICET, UNSAM), Buenos Aires, Argentina
[8] International Center of Advanced Studies and Instituto de Ciencias Físicas, ECyT-UNSAM and CONICET, Campus Miguelete – San Martín, Buenos Aires, Argentina
[9] Laboratorio Atmósfera – Departamento de Investigaciones en Láseres y sus Aplicaciones – UNIDEF (CITEDEF-CONICET), Argentina
[10] Observatorio Pierre Auger, Malargüe, Argentina
[11] Observatorio Pierre Auger and Comisión Nacional de Energía Atómica, Malargüe, Argentina
[12] Universidad Tecnológica Nacional – Facultad Regional Buenos Aires, Buenos Aires, Argentina
[13] University of Adelaide, Adelaide, S.A., Australia
[14] Université Libre de Bruxelles (ULB), Brussels, Belgium
[15] Vrije Universiteit Brussels, Brussels, Belgium
[16] Centro Federal de Educação Tecnológica Celso Suckow da Fonseca, Petropolis, Brazil
[17] Instituto Federal de Educação, Ciência e Tecnologia do Rio de Janeiro (IFRJ), Brazil
[18] Universidade de São Paulo, Escola de Engenharia de Lorena, Lorena, SP, Brazil
[19] Universidade de São Paulo, Instituto de Física de São Carlos, São Carlos, SP, Brazil
[20] Universidade de São Paulo, Instituto de Física, São Paulo, SP, Brazil
[21] Universidade Estadual de Campinas, IFGW, Campinas, SP, Brazil
[22] Universidade Estadual de Feira de Santana, Feira de Santana, Brazil
[23] Universidade Federal de Campina Grande, Centro de Ciencias e Tecnologia, Campina Grande, Brazil
[24] Universidade Federal do ABC, Santo André, SP, Brazil
[25] Universidade Federal do Paraná, Setor Palotina, Palotina, Brazil
[26] Universidade Federal do Rio de Janeiro, Instituto de Física, Rio de Janeiro, RJ, Brazil
[27] Universidade Federal do Rio de Janeiro (UFRJ), Observatório do Valongo, Rio de Janeiro, RJ, Brazil
[28] Universidade Federal Fluminense, EEIMVR, Volta Redonda, RJ, Brazil
[29] Universidad de Medellín, Medellín, Colombia
[30] Universidad Industrial de Santander, Bucaramanga, Colombia

[31] Charles University, Faculty of Mathematics and Physics, Institute of Particle and Nuclear Physics, Prague, Czech Republic
[32] Institute of Physics of the Czech Academy of Sciences, Prague, Czech Republic
[33] Palacky University, Olomouc, Czech Republic
[34] CNRS/IN2P3, IJCLab, Université Paris-Saclay, Orsay, France
[35] Laboratoire de Physique Nucléaire et de Hautes Energies (LPNHE), Sorbonne Université, Université de Paris, CNRS-IN2P3, Paris, France
[36] Univ. Grenoble Alpes, CNRS, Grenoble Institute of Engineering Univ. Grenoble Alpes, LPSC-IN2P3, 38000 Grenoble, France
[37] Université Paris-Saclay, CNRS/IN2P3, IJCLab, Orsay, France
[38] Bergische Universität Wuppertal, Department of Physics, Wuppertal, Germany
[39] Karlsruhe Institute of Technology (KIT), Institute for Experimental Particle Physics, Karlsruhe, Germany
[40] Karlsruhe Institute of Technology (KIT), Institut für Prozessdatenverarbeitung und Elektronik, Karlsruhe, Germany
[41] Karlsruhe Institute of Technology (KIT), Institute for Astroparticle Physics, Karlsruhe, Germany
[42] RWTH Aachen University, III. Physikalisches Institut A, Aachen, Germany
[43] Universität Hamburg, II. Institut für Theoretische Physik, Hamburg, Germany
[44] Universität Siegen, Department Physik – Experimentelle Teilchenphysik, Siegen, Germany
[45] Gran Sasso Science Institute, L'Aquila, Italy
[46] INFN Laboratori Nazionali del Gran Sasso, Assergi (L'Aquila), Italy
[47] INFN, Sezione di Catania, Catania, Italy
[48] INFN, Sezione di Lecce, Lecce, Italy
[49] INFN, Sezione di Milano, Milano, Italy
[50] INFN, Sezione di Napoli, Napoli, Italy
[51] INFN, Sezione di Roma "Tor Vergata", Roma, Italy
[52] INFN, Sezione di Torino, Torino, Italy
[53] Istituto di Astrofisica Spaziale e Fisica Cosmica di Palermo (INAF), Palermo, Italy
[54] Osservatorio Astrofisico di Torino (INAF), Torino, Italy
[55] Politecnico di Milano, Dipartimento di Scienze e Tecnologie Aerospaziali , Milano, Italy
[56] Università del Salento, Dipartimento di Matematica e Fisica "E. De Giorgi", Lecce, Italy
[57] Università dell'Aquila, Dipartimento di Scienze Fisiche e Chimiche, L'Aquila, Italy
[58] Università di Catania, Dipartimento di Fisica e Astronomia "Ettore Majorana", Catania, Italy
[59] Università di Milano, Dipartimento di Fisica, Milano, Italy
[60] Università di Napoli "Federico II", Dipartimento di Fisica "Ettore Pancini", Napoli, Italy
[61] Università di Palermo, Dipartimento di Fisica e Chimica "E. Segrè", Palermo, Italy
[62] Università di Roma "Tor Vergata", Dipartimento di Fisica, Roma, Italy
[63] Università Torino, Dipartimento di Fisica, Torino, Italy
[64] Benemérita Universidad Autónoma de Puebla, Puebla, México
[65] Unidad Profesional Interdisciplinaria en Ingeniería y Tecnologías Avanzadas del Instituto Politécnico Nacional (UPIITA-IPN), México, D.F., México
[66] Universidad Autónoma de Chiapas, Tuxtla Gutiérrez, Chiapas, México
[67] Universidad Michoacana de San Nicolás de Hidalgo, Morelia, Michoacán, México
[68] Universidad Nacional Autónoma de México, México, D.F., México
[69] Universidad Nacional de San Agustin de Arequipa, Facultad de Ciencias Naturales y Formales, Arequipa, Peru
[70] Institute of Nuclear Physics PAN, Krakow, Poland
[71] University of Łódź, Faculty of High-Energy Astrophysics,Łódź, Poland
[72] Laboratório de Instrumentação e Física Experimental de Partículas – LIP and Instituto Superior Técnico – IST, Universidade de Lisboa – UL, Lisboa, Portugal
[73] "Horia Hulubei" National Institute for Physics and Nuclear Engineering, Bucharest-Magurele, Romania
[74] Institute of Space Science, Bucharest-Magurele, Romania
[75] University Politehnica of Bucharest, Bucharest, Romania
[76] Center for Astrophysics and Cosmology (CAC), University of Nova Gorica, Nova Gorica, Slovenia
[77] Experimental Particle Physics Department, J. Stefan Institute, Ljubljana, Slovenia

PoS(ICRC2023)1095

[78] Universidad de Granada and C.A.F.P.E., Granada, Spain
[79] Instituto Galego de Física de Altas Enerxías (IGFAE), Universidade de Santiago de Compostela, Santiago de Compostela, Spain
[80] IMAPP, Radboud University Nijmegen, Nijmegen, The Netherlands
[81] Nationaal Instituut voor Kernfysica en Hoge Energie Fysica (NIKHEF), Science Park, Amsterdam, The Netherlands
[82] Stichting Astronomisch Onderzoek in Nederland (ASTRON), Dwingeloo, The Netherlands
[83] Universiteit van Amsterdam, Faculty of Science, Amsterdam, The Netherlands
[84] Case Western Reserve University, Cleveland, OH, USA
[85] Colorado School of Mines, Golden, CO, USA
[86] Department of Physics and Astronomy, Lehman College, City University of New York, Bronx, NY, USA
[87] Michigan Technological University, Houghton, MI, USA
[88] New York University, New York, NY, USA
[89] University of Chicago, Enrico Fermi Institute, Chicago, IL, USA
[90] University of Delaware, Department of Physics and Astronomy, Bartol Research Institute, Newark, DE, USA
[91] University of Wisconsin-Madison, Department of Physics and WIPAC, Madison, WI, USA

—

[a] Louisiana State University, Baton Rouge, LA, USA
[b] also at University of Bucharest, Physics Department, Bucharest, Romania
[c] School of Physics and Astronomy, University of Leeds, Leeds, United Kingdom
[d] now at Agenzia Spaziale Italiana (ASI). Via del Politecnico 00133, Roma, Italy
[e] Fermi National Accelerator Laboratory, Fermilab, Batavia, IL, USA
[f] now at Graduate School of Science, Osaka Metropolitan University, Osaka, Japan
[g] now at ECAP, Erlangen, Germany
[h] Max-Planck-Institut für Radioastronomie, Bonn, Germany
[i] also at Kapteyn Institute, University of Groningen, Groningen, The Netherlands
[j] Colorado State University, Fort Collins, CO, USA
[k] Pennsylvania State University, University Park, PA, USA

Acknowledgments

The successful installation, commissioning, and operation of the Pierre Auger Observatory would not have been possible without the strong commitment and effort from the technical and administrative staff in Malargüe. We are very grateful to the following agencies and organizations for financial support:

Argentina – Comisión Nacional de Energía Atómica; Agencia Nacional de Promoción Científica y Tecnológica (ANPCyT); Consejo Nacional de Investigaciones Científicas y Técnicas (CONICET); Gobierno de la Provincia de Mendoza; Municipalidad de Malargüe; NDM Holdings and Valle Las Leñas; in gratitude for their continuing cooperation over land access; Australia – the Australian Research Council; Belgium – Fonds de la Recherche Scientifique (FNRS); Research Foundation Flanders (FWO); Brazil – Conselho Nacional de Desenvolvimento Científico e Tecnológico (CNPq); Financiadora de Estudos e Projetos (FINEP); Fundação de Amparo à Pesquisa do Estado de Rio de Janeiro (FAPERJ); São Paulo Research Foundation (FAPESP) Grants No. 2019/10151-2, No. 2010/07359-6 and No. 1999/05404-3; Ministério da Ciência, Tecnologia, Inovações e Comunicações (MCTIC); Czech Republic – Grant No. MSMT CR LTT18004, LM2015038, LM2018102, CZ.02.1.01/0.0/0.0/16_013/0001402, CZ.02.1.01/0.0/0.0/18_046/0016010 and CZ.02.1.01/0.0/0.0/17_049/0008422; France – Centre de Calcul IN2P3/CNRS; Centre National de la Recherche Scientifique (CNRS); Conseil Régional Ile-de-France; Département Physique Nucléaire et Corpusculaire (PNC-IN2P3/CNRS); Département Sciences de l'Univers (SDU-INSU/CNRS); Institut Lagrange de Paris (ILP) Grant No. LABEX ANR-10-LABX-63 within the Investissements d'Avenir Programme Grant No. ANR-11-IDEX-0004-02; Germany – Bundesministerium für Bildung und Forschung (BMBF); Deutsche Forschungsgemeinschaft (DFG); Finanzministerium Baden-Württemberg; Helmholtz Alliance for Astroparticle Physics (HAP); Helmholtz-Gemeinschaft Deutscher Forschungszentren (HGF); Ministerium für Kultur und Wissenschaft des Landes Nordrhein-Westfalen; Ministerium für Wissenschaft, Forschung und Kunst des Landes Baden-Württemberg; Italy – Istituto Nazionale di Fisica Nucleare (INFN); Istituto Nazionale di Astrofisica (INAF); Ministero dell'Universitá e della Ricerca (MUR); CETEMPS Center of Excellence; Ministero degli Affari Esteri (MAE), ICSC Centro Nazionale di Ricerca in High Performance Computing, Big Data

and Quantum Computing, funded by European Union NextGenerationEU, reference code CN_00000013; México – Consejo Nacional de Ciencia y Tecnología (CONACYT) No. 167733; Universidad Nacional Autónoma de México (UNAM); PAPIIT DGAPA-UNAM; The Netherlands – Ministry of Education, Culture and Science; Netherlands Organisation for Scientific Research (NWO); Dutch national e-infrastructure with the support of SURF Cooperative; Poland – Ministry of Education and Science, grants No. DIR/WK/2018/11 and 2022/WK/12; National Science Centre, grants No. 2016/22/M/ST9/00198, 2016/23/B/ST9/01635, 2020/39/B/ST9/01398, and 2022/45/B/ST9/02163; Portugal – Portuguese national funds and FEDER funds within Programa Operacional Factores de Competitividade through Fundação para a Ciência e a Tecnologia (COMPETE); Romania – Ministry of Research, Innovation and Digitization, CNCS-UEFISCDI, contract no. 30N/2023 under Romanian National Core Program LAPLAS VII, grant no. PN 23 21 01 02 and project number PN-III-P1-1.1-TE-2021-0924/TE57/2022, within PNCDI III; Slovenia – Slovenian Research Agency, grants P1-0031, P1-0385, I0-0033, N1-0111; Spain – Ministerio de Economía, Industria y Competitividad (FPA2017-85114-P and PID2019-104676GB-C32), Xunta de Galicia (ED431C 2017/07), Junta de Andalucía (SOMM17/6104/UGR, P18-FR-4314) Feder Funds, RENATA Red Nacional Temática de Astropartículas (FPA2015-68783-REDT) and María de Maeztu Unit of Excellence (MDM-2016-0692); USA – Department of Energy, Contracts No. DE-AC02-07CH11359, No. DE-FR02-04ER41300, No. DE-FG02-99ER41107 and No. DE-SC0011689; National Science Foundation, Grant No. 0450696; The Grainger Foundation; Marie Curie-IRSES/EPLANET; European Particle Physics Latin American Network; and UNESCO.